THE JOURNAL OF
PHYSICAL CHEMISTRY
LETTERS
A JOURNAL OF THE AMERICAN CHEMICAL SOCIETY

May 9, 2024
Volume 15
Number 18
pubs.acs.org/JPCL

ACS Publications
Most Trusted. Most Cited. Most Read.

www.acs.org

THE JOURNAL OF PHYSICAL CHEMISTRY LETTERS
A JOURNAL OF THE AMERICAN CHEMICAL SOCIETY

pubs.acs.org/JPCL
Letter

How Does the Antibiotic Amphotericin B Enter Membranes and What Does It Do There?

Sebastian Janik, Rafal Luchowski, Ewa Grela, Wojciech Grudzinski, and Wieslaw I. Gruszecki*

Cite This: J. Phys. Chem. Lett. 2024, 15, 4823−4827
Read Online

ABSTRACT: Amphotericin B is a popular antifungal antibiotic, but the exact way it works is still a matter of debate. Here, we used monolayers composed of phosphatidylcholine with ergosterol as a model of fungal lipid membranes to study drug incorporation from the aqueous phase and analyze the molecular reorganization of membranes underlying the biological activity of the antibiotic. The results show that the internalization of antibiotic molecules into membranes occurs only in the presence of ergosterol in the lipid phase. Comparison of images of solid-supported monolayers obtained by atomic force microscopy and lifetime imaging fluorescence microscopy shows the formation of intramembrane clusters of various sizes in the lipid phase, consisting mainly of antibiotic dimers and relatively large membrane pores (∼15 nm in diameter). The results reveal multiple modes of action of amphotericin B, acting simultaneously, each of which adversely affects the structural properties of the lipid membranes and their physiological functionality.

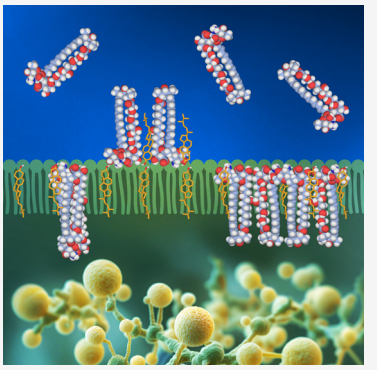

Amphotericin B (AmB) belongs to a class of polyene macrolide antibiotics and is used to treat deep-seated, life-threatening fungal infections[1,2] (see Supplementary Figure S1 for a chemical structure). Paradoxically, despite several decades of medical use of AmB and its high effectiveness,[3] the exact modes of its biological activity are still a matter of debate.[4,5] Among the main mechanisms discussed is the destabilization of a structure of biomembranes, induced by the presence of the drug molecules in the lipid phase[6,7] or as a consequence of the sequestration of sterols associated with the formation of extramembraneous sterol-AmB bulk structures referred to as "sponges".[8,9] One of the consequences of the destabilization of the membrane structure would be the uncontrolled leakage of physiologically important ions through the biomembranes, disturbing the electrostasis of living cells. Another important mechanism underlying the antibiotic action of AmB is the formation of transmembrane pores that act as passive ion channels uncontrolled by any regulatory activity,[10] thus also having a decidedly negative impact on physiological ion transport. Currently, there are two models of barrel-stave-like transmembrane ion channels formed by AmB molecules in the lipid phase: one composed of a single-length complex[11] and the other consisting of a double-length channel formed by two stacked single-length structures, each present in a single leaflet of the lipid bilayer.[12] In the opinion of many researchers, the results of the experiments supporting all of the individual modes of action of AmB concerning lipid membranes are convincing, thus making it difficult to sort out which molecular mechanism applies to the pharmacological effect of this antibiotic. In the present work, we designed experiments in combination with various imaging techniques to further address this interesting issue, important from the point of view of designing future formulations of this drug that are characterized by minimized toxic side effects for patients. We used a model system of monomolecular layers formed at the air−water interface with dioleoylphosphatidylcholine (DOPC) and ergosterol (Ergo), the main sterol of fungal cells, to study the incorporation of drug molecules into the membrane from the water phase.[13] Monolayers deposited on a solid support were then subjected to functional imaging. The main advantage of using atomic force microscopy (AFM) was the very high spatial resolution of this technique, while the use of fluorescence lifetime imaging microscopy (FLIM) was advantageous due to the sensitivity of fluorescence lifetime parameters to the molecular organization of AmB.[14] The use of various imaging techniques in studying the interactions of pharmacologically active molecules with membranes has proven to be highly effective in understanding the mechanisms of their biological activity.[15−17] Surprisingly, the results obtained in this study demonstrate multiple modes of action of AmB on lipid membranes, all of which may account for the pharmacological effectiveness of this popular antibiotic.

Figure 1 presents a FLIM image of a film deposited from the single DOPC-Ergo monolayer formed at the air−water interface and exposed to AmB that was introduced into the

Received: February 16, 2024
Revised: March 29, 2024
Accepted: April 22, 2024
Published: April 26, 2024

https://doi.org/10.1021/acs.jpclett.4c00496
J. Phys. Chem. Lett. 2024, 15, 4823−4827

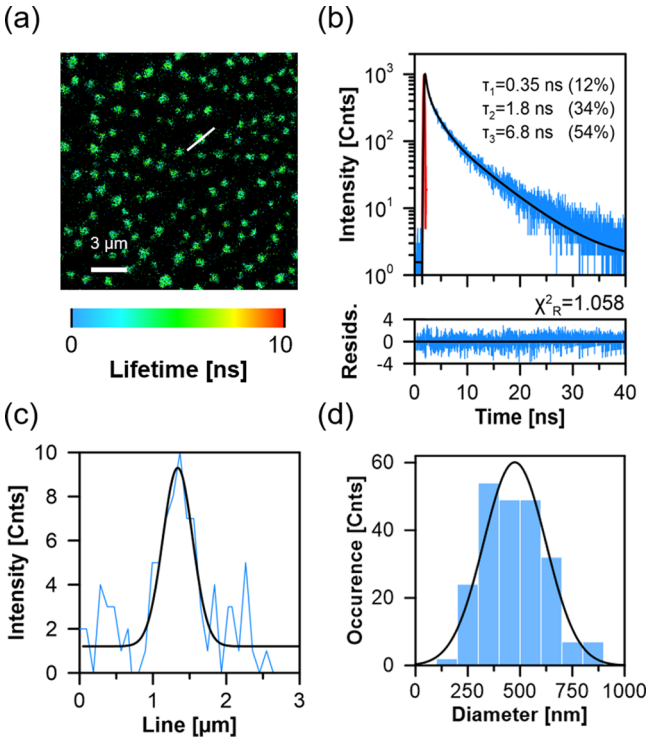

Figure 1. FLIM image and analysis of the film deposited from the monomolecular layer composed of DOPC and Ergo (7:3) exposed to AmB. (a) FLIM image, (b) fluorescence lifetime analysis based on all the photons detected during the imaging (IRF plotted in red), (c) cross-section analysis along the structure marked in panel (a) with white line, and (d) analysis of diameters of the fluorescence-emitting structures visible in panel (a) and another four images and based on the *fwhh* of fits to the signal as shown in panel (c). See the text for more information. The figure shows analyses of the exact same sample that was analyzed using AFM (results shown in Figure 2).

water subphase. The fluorescence signal assigned to AmB shows the incorporation of the drug molecules into the lipid phase.[18] The fluorescence signal of this polyene antibiotic can be effectively detected despite the low concentration in the monolayer system, thanks to the relatively high fluorescence quantum yield of AmB (~4% in the dimeric form[19]) and the very high sensitivity of the detection system. The fluorescence emission spectra of AmB incorporated into monolayers are presented in the Supplementary Figure S2. The position of the fluorescence emission band on the wavelength scale suggests that AmB present in the system examined appears mostly in the form of dimers and small molecular aggregates.[14] AmB fluorescence has not been detected in the same experiment carried out under identical conditions, except that Ergo molecules were not present in the lipid monolayer (see Supplementary Figure S3). This result confirms that the presence of sterols, in particular ergosterol, in the system is a prerequisite for the effective penetration of AmB from the aqueous phase into lipid membranes.[18] Detailed analysis of the FLIM image (Figure 1) shows that AmB incorporated in the DOPC-Ergo membrane is not distributed homogeneously but rather self-associates into clusters characterized by dimensions in the range of 250−750 nm. The spatial resolution of the optical microscopic system used enabled the discrimination of structures with a minimum dimension of 226 ± 27 nm (see the Supporting Information for experimental details). It is therefore highly probable that exact dimensions of the smallest molecular structures formed are significantly lower. The time-resolved fluorescence analysis shows that AmB in the system appears in three molecular organization forms characterized by the fluorescence lifetimes τ_1 = 0.35 ns (12%), τ_2 = 1.8 ns (34%), and τ_3 = 6.8 ns (54%), assigned to small aggregates (e.g., tetramers), parallel dimers, and antiparallel dimers, respectively.[14] Importantly, the amplitudes of the AmB fluorescence lifetime components in the monolayer show that the antibiotic does not exist as a monomer and that dimers are the main forms of molecular organization in this system. This observation suggests that other molecules, including a sterol and possibly also a lipid, are involved in the formation of the relatively large AmB clusters observed, presumably serving as "molecular spacers" protecting against strong excitonic interactions between chromophores. Interestingly, such large structures are not distinguished in the AFM images of multicomponent monolayers (Figure 2). This suggests that

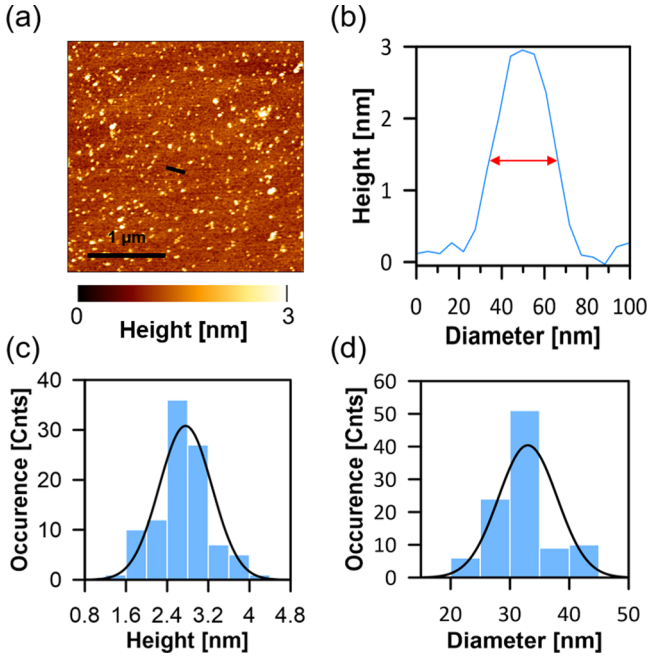

Figure 2. AFM image and analysis of the film deposited from the monomolecular layer composed of DOPC and Ergo (7:3) exposed to AmB. (a) AFM image, (b) cross-section analysis along the black line marked in panel (a), and analysis of height (c) and diameter (d) of the structures appearing as white dots in the image presented in panel (a), according to the methodology presented in panel b. The figure shows analyses of the exact same sample that was analyzed using FLIM (results shown in Figure 1).

some AmB structures separated by a relatively short distance can be resolved using the AFM technique but are recognized as single larger objects by the optical imaging. On the other hand, AFM-based images show the presence of relatively small structures (20−50 nm in diameter) distinctly differing in height above the level of the monolayer (~3 nm, corresponding to the length of a single AmB molecule[20]). The pillar-like structures visible in the film topography are also distinctly different from the membranes in nanomechanical properties, as can be concluded from the sample imaging based on the AFM phase signal (see Supplementary Figure S4). In principle, such structures can be formed at the water−membrane interface and, thanks to their stability, remain

https://doi.org/10.1021/acs.jpclett.4c00496
J. Phys. Chem. Lett. 2024, 15, 4823−4827

preserved in the process of the deposition of monolayers on a solid support. The fact that such structures are not observed for lipid monolayers exposed to AmB but lacking Ergo (Supplementary Figure S3) suggests that sterol molecules are not only necessary for the internalization of AmB into the membrane but are also involved in the formation of the bulk structures detected using a topography imaging of the samples. More detailed analysis of the AFM images also reveals the appearance of relatively small depressions in the membrane, manifested as black dots (Figure 3). Such structures are typical

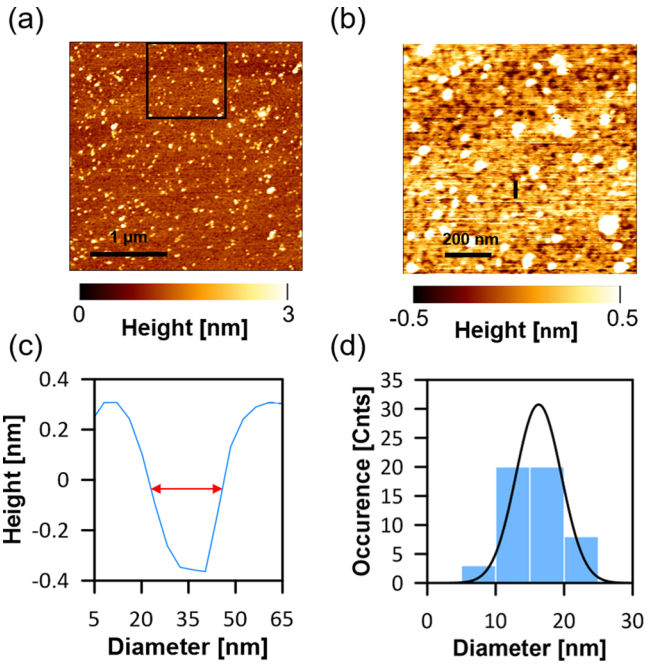

Figure 3. AFM image and analysis of the film deposited from the monomolecular layer composed of DOPC and Ergo (7:3) exposed to AmB. (a) AFM image, (b) detailed analysis of the image marked in panel a with black square, (c) cross-section analysis along the black line marked in panel (b), and (d) analysis of a diameter of the structures appearing as black dots in the image presented in panel (b), according to the methodology presented in panel (c).

for the lipid monolayers containing Ergo and exposed to AmB. The diameters of such structures (~15 nm) are too large to be considered as single ion channels, but certainly, they have the potential to act as pores significantly affecting the membrane structure and disturbing physiological ion transport. Despite the fact that the diameters of pillar-like structures (Figure 2) are larger than those of pore-like structures (Figure 3), it is possible that both types of structures may have the same origin: namely, they are formed in the separation process from membrane clusters rich in AmB and Ergo. The observed differences in diameter can be related both to the molecular dynamics of the multicomponent membrane and the process of relaxation after the emergence of new structures as well as to the different detection of convex structures and cavities using the AFM technique.

The results of the analysis indicate the occurrence of various forms of molecular organization associated with the exposure of the lipid membrane containing Ergo to the action of AmB. First, AmB-related effects are observed only in sterol-containing lipid membranes. Such observations are in agreement with the results of the previous studies showing that sterols are necessary components of membranes that allow AmB molecules to penetrate into the lipid phase and ensure vertical orientation of the antibiotic molecules, along the axis perpendicular to the membrane plane.[18,21] In the present study, two essentially different forms of AmB molecular organization in the membrane were observed, important from the standpoint of the structure–function relationship: intramembrane clusters separated from the lipid phase (20 to 50 nm in diameter) and ~15 nm pores (see Figure 4 for a

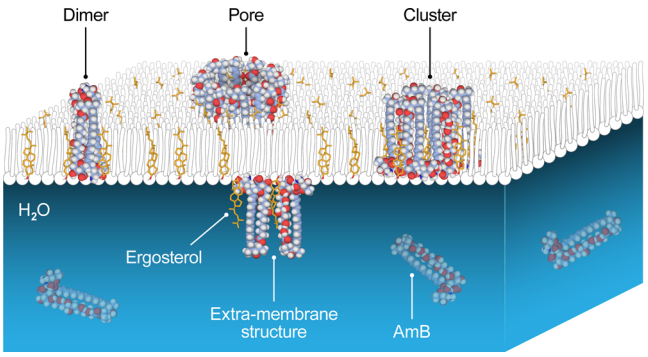

Figure 4. Model illustrating the process of internalization of AmB into the DOPC-Ergo monolayer from the aqueous subphase and the formation of various molecular structures.

visualization). Importantly, AmB does not appear as a monomer but adopts more complex forms with the dimeric suborganization. It is concluded that the membrane components, presumably lipids and sterols, participate in the formation and stabilization of the observed structures. In our opinion, all these forms of molecular organization of AmB significantly influence the structural properties of biomembranes, which are important from a physiological point of view. Membrane phase separation, appearing as AmB-rich clusters, generates interfacial boundaries that may facilitate uncontrolled transmembrane transport of small molecules, including ions. An even greater risk of this process can be expected in the presence of membrane pores. The formation of extramembrane structures also seems to be important from a biological point of view. They likely represent molecular organization forms identified previously as sterol-rich AmB "sponges". The results of model system studies presented in this work show that the presence of AmB in a lipid membrane containing sterols results in many consequences at the level of molecular organization and structural properties of membranes. Importantly, all of them may impair their biological functionality. This leads to the conclusion that the problem of the molecular basis of the pharmacological action of AmB is complex and is not limited to only one mechanism. Although the present study has revealed several effects of AmB on membranes, we are aware that due to the specificity of the techniques used and their resolution, several other potential mechanisms may not have been observed, e.g., the formation of very small ion channels. Apparently, the relatively complex and specific molecular structure of AmB itself modulates a whole series of interactions in the membrane environment, causing its significant reorganization, which manifests itself in many different ways depending on the research technique used.

https://doi.org/10.1021/acs.jpclett.4c00496
J. Phys. Chem. Lett. 2024, 15, 4823–4827

■ ASSOCIATED CONTENT

Supporting Information

The Supporting Information is available free of charge at https://pubs.acs.org/doi/10.1021/acs.jpclett.4c00496.

Experimental details, chemical structure of amphotericin B, fluorescence emission spectrum of AmB incorporated into the lipid monolayer, AFM image based on the phase signal, AFM and FLIM images of the DOPC monolayers lacking Ergo and exposed to AmB, and isotherm of compression of the DOPC-Ergo monomolecular layer (PDF)

■ AUTHOR INFORMATION

Corresponding Author

Wieslaw I. Gruszecki − *Department of Biophysics, Institute of Physics, Maria Curie-Sklodowska University, 20-031 Lublin, Poland;* orcid.org/0000-0002-8245-3913; Email: wieslaw.gruszecki@umcs.pl

Authors

Sebastian Janik − *Department of Biophysics, Institute of Physics, Maria Curie-Sklodowska University, 20-031 Lublin, Poland*

Rafal Luchowski − *Department of Biophysics, Institute of Physics, Maria Curie-Sklodowska University, 20-031 Lublin, Poland; Department of Biophysics, Medical University of Lublin, 20-059 Lublin, Poland;* orcid.org/0000-0003-1156-8059

Ewa Grela − *Department of Biophysics, Institute of Physics, Maria Curie-Sklodowska University, 20-031 Lublin, Poland; Division of Biophysics, Institute of Experimental Physics, Faculty of Physics, University of Warsaw, 02-093 Warsaw, Poland;* orcid.org/0000-0002-1667-6780

Wojciech Grudzinski − *Department of Biophysics, Institute of Physics, Maria Curie-Sklodowska University, 20-031 Lublin, Poland;* orcid.org/0000-0002-8825-1423

Complete contact information is available at: https://pubs.acs.org/10.1021/acs.jpclett.4c00496

Notes

The authors declare no competing financial interest.

■ ACKNOWLEDGMENTS

The authors dedicate this work to the memory of our friend and co-worker Dr. Peter Kernen. The National Science Center of Poland (NCN) is acknowledged for the financial support within the Project 2019/33/B/NZ7/00902.

■ REFERENCES

(1) Mesa-Arango, A. C.; Scorzoni, L.; Zaragoza, O. It only takes one to do many jobs: Amphotericin B as antifungal and immunomodulatory drug. *Front. Microbiol.* **2012**, DOI: 10.3389/fmicb.2012.00286.

(2) Dismukes, W. E. Antifungal therapy: Lessons learned over the past 27 years. *Clin. Infect. Dis.* **2006**, *42* (9), 1289−1296.

(3) Cavassin, F. B.; Bau-Carneiro, J. L.; Vilas-Boas, R. R.; Queiroz-Telles, F. Sixty years of Amphotericin B: An Overview of the Main Antifungal Agent Used to Treat Invasive Fungal Infections. *Infect. Dis. Ther.* **2021**, *10* (1), 115−147.

(4) Carolus, H.; Pierson, S.; Lagrou, K.; Van Dijck, P. Amphotericin B and Other Polyenes-Discovery, Clinical Use, Mode of Action and Drug Resistance. *J. Fungi* **2020**, *6* (4), 321.

(5) Grela, E.; Zdybicka-Barabas, A.; Pawlikowska-Pawlega, B.; Cytrynska, M.; Wlodarczyk, M.; Grudzinski, W.; Luchowski, R.; Gruszecki, W. I. Modes of the antibiotic activity of amphotericin B against Candida albicans. *Sci. Rep.* **2019**, *9*, 17029.

(6) Herec, M.; Islamov, A.; Kuklin, A.; Gagos, M.; Gruszecki, W. I. Effect of antibiotic amphotericin B on structural and dynamic properties of lipid membranes formed with egg yolk phosphatidylcholine. *Chem. Phys. Lipids* **2007**, *147* (2), 78−86.

(7) Grela, E.; Wieczor, M.; Luchowski, R.; Zielinska, J.; Barzycka, A.; Grudzinski, W.; Nowak, K.; Tarkowski, P.; Czub, J.; Gruszecki, W. I. A mechanism of binding of an antifungal antibiotic amphotericin B to lipid membranes: An insight from combined single membrane imaging, micro-spectroscopy, and molecular dynamics. *Mol. Pharmaceutics* **2018**, *15*, 4202−4213.

(8) Anderson, T. M.; Clay, M. C.; Cioffi, A. G.; Diaz, K. A.; Hisao, G. S.; Tuttle, M. D.; Nieuwkoop, A. J.; Comellas, G.; Maryum, N.; Wang, S.; et al. Amphotericin forms an extramembranous and fungicidal sterol sponge. *Nat. Chem. Biol.* **2014**, *10* (5), 400−406.

(9) Lewandowska, A.; Soutar, C. P.; Greenwood, A. I.; Nimerovsky, E.; De Lio, A. M.; Holler, J. T.; Hisao, G. S.; Khandelwal, A.; Zhang, J. B.; SantaMaria, A. M.; et al. Fungicidal amphotericin B sponges are assemblies of staggered asymmetric homodimers encasing large void volumes. *Nat. Struct. Mol. Biol.* **2021**, *28* (12), 972−981.

(10) De Kruijff, B.; Demel, R. A. Polyene antibiotic-sterol interaction in membranes of *Acholeplasma laidlawii* cells and lecithin liposomes; III Molecular structure of the polyene antibiotic-cholesterol complex. *Biochim. Biophys. Acta* **1974**, *339*, 57−70.

(11) Yamamoto, T.; Umegawa, Y.; Tsuchikawa, H.; Hanashima, S.; Matsumori, N.; Funahashi, K.; Seo, S.; Shinoda, W.; Murata, M. The Amphotericin B-Ergosterol Complex Spans a Lipid Bilayer as a Single-Length Assembly. *Biochemistry* **2019**, *58* (51), 5188−5196.

(12) Zielinska, J.; Wieczor, M.; Chodnicki, P.; Grela, E.; Luchowski, R.; Nierzwicki, L.; Baczek, T.; Gruszecki, W. I.; Czub, J. Self-assembly, stability and conductance of amphotericin B channels: bridging the gap between structure and function. *Nanoscale* **2021**, *13*, 3686.

(13) Gagos, M.; Gabrielska, J.; Dalla Serra, M.; Gruszecki, W. I. Binding of antibiotic amphotericin B to lipid membranes: monomolecular layer technique and linear dichroism-FTIR studies. *Mol. Membr. Biol.* **2005**, *22* (5), 433−442.

(14) Starzyk, J.; Gruszecki, M.; Tutaj, K.; Luchowski, R.; Szlazak, R.; Wasko, P.; Grudzinski, W.; Czub, J.; Gruszecki, W. I. Self-association of amphotericin B: spontaneous formation of molecular structures responsible for the toxic side effects of the antibiotic. *J. Phys. Chem. B* **2014**, *118*, 13821−13832.

(15) Mescola, A.; Ragazzini, G.; Facci, P.; Alessandrini, A. The potential of AFM in studying the role of the nanoscale amphipathic nature of (lipo)-peptides interacting with lipid bilayers. *Nanotechnology* **2022**, *33* (43), 432001.

(16) Datta, R.; Heaster, T. M.; Sharick, J. T.; Gillette, A. A.; Skala, M. C. Fluorescence lifetime imaging microscopy: fundamentals and advances in instrumentation, analysis, and applications. *J. Biomed Opt* **2020**, *25* (7), 071203.

(17) Balleza, D.; Mescola, A.; Alessandrini, A. Model lipid systems and their use to evaluate the phase state of biomembranes, their mechanical properties and the effect of non-conventional antibiotics: the case of daptomycin. *Eur. Biophys J. Biophy* **2020**, *49* (5), 401−408.

(18) Grudzinski, W.; Sagan, J.; Welc, R.; Luchowski, R.; Gruszecki, W. I. Molecular organization, localization and orientation of antifungal antibiotic amphotericin B in a single lipid bilayer. *Sci. Rep.* **2016**, *6*, 32780.

(19) Gruszecki, W. I.; Gagos, M.; Herec, M. Dimers of polyene antibiotic amphotericin B detected by means of fluorescence spectroscopy: molecular organization in solution and in lipid membranes. *J. Photoch Photobio B* **2003**, *69* (1), 49−57.

(20) Jarzembska, K. N.; Kaminski, D.; Hoser, A. A.; Malinska, M.; Senczyna, B.; Wozniak, K.; Gagos, M. Controlled Crystallization, Structure, and Molecular Properties of Iodoacetylamphotericin B. *Cryst. Growth Des.* **2012**, *12* (5), 2336−2345.

(21) Dong, P. T.; Zong, C.; Dagher, Z.; Hui, J.; Li, J. J.; Zhan, Y. W.; Zhang, M.; Mansour, M. K.; Cheng, J. X. Polarization-sensitive

stimulated Raman scattering imaging resolves amphotericin B orientation in membrane. *Sci. Adv.* **2021**, *7* (2), eabd5230.

https://doi.org/10.1021/acs.jpclett.4c00496
J. Phys. Chem. Lett. 2024, 15, 4823−4827

Supporting Information

How does the Antibiotic Amphotericin B Enter Membranes and What does it Do There?

Sebastian Janik[a], *Rafal Luchowski*[a,b], *Ewa Grela*[a,c], *Wojciech Grudzinski*[a], *and Wieslaw I. Gruszecki*[a,*]

[a] *Department of Biophysics, Institute of Physics, Maria Curie-Sklodowska University, 20-031 Lublin, Poland*

[b] *Department of Biophysics, Medical University of Lublin, 20-059 Lublin, Poland*

[c] *Division of Biophysics, Institute of Experimental Physics, Faculty of Physics, University of Warsaw, 02-093 Warsaw, Poland*

[*] corresponding author: wieslaw.gruszecki@umcs.pl

Experimental Section

Materials

Crystalline amphotericin B (AmB) was purchased from Cayman Chemical (USA). Directly before use, AmB was repurified chromatographically, as described in detail previously.[1] 1,2-dioleoyl-sn-glycero-3-phosphocholine (DOPC) was obtained from Avanti Polar Lipids (USA). Ergosterol was obtained from Merck (Germany). Methanol, 2-propanol and chloroform were purchased from POCH (Poland). Water used in experiments was purified by a Milli-Q Millipore system (Merck, Germany).

Preparation of monomolecular layers

Monomolecular layers were formed using a Teflon trough equipped with movable barriers, an injection port, and a magnetic stirrer. An integrated Langmuir and Langmuir-Blodgett system was purchased from KSV NIMA Instruments (Finland). A Wilhelmy tensiometer with an ashless filter paper (Whatman) as a surface pressure sensor was used to monitor surface pressure. Before starting the main part of the experiment, the DOPC:Ergo (7:3, mol:mol) monolayers were formed at the air-water interface and isotherms of compression were recorded (See Supporting Information Figure S5). A monolayer constituents were deposited at the air-water interface in 50 µl of a DOPC and Ergo solution prepared in a chloroform:methanol (9:1, v/v) solvent mixture. The monolayer compression began after 15 min. necessary for solvent evaporation. The barrier speed was constant at 10 mm/min. To examine the penetration of AmB from the water phase into the lipid monolayers, the films were compressed to 25 mN/m, and this surface pressure was stabilized automatically by the computer-controlled system. AmB was injected into the aqueous subphase, beneath the monomolecular layers, as a solution prepared in water/2-propanol mixture (6:4, v/v). A volume of 100 µl of AmB solution was injected into

~300 ml of water subphase. The concentration of AmB solution was adjusted to maintain the 1:1 ratio of molecules of AmB in the subphase and the total number of DOPC and Ergo molecules forming the lipid monolayers. The process of incorporation of AmB into the monolayers was manifested by a computer-controlled decompression of the films to maintain the surface pressure at 25 mN/m. After stabilization of this process (40 min.), the monomolecular layers were transferred to freshly cleaved Mica substrate by means of the Langmuir-Blodgett technique. The same constant surface pressure was automatically maintained by the system, also during the process of deposition of monomolecular films to a solid support. All experiments were performed at 25 °C. Single-component and multicomponent monomolecular layers formed with AmB, lipids, and sterols were characterized in detail in our previous studies.[2]

Atomic Force Microscopy

The monolayers were deposited on a freshly cleaved Mica surface at room temperature and then transferred to an AFM microscope. AFM scanning was carried out using JPK Nanowizard 3 system (Bruker, USA) in a non-contact mode (AC mode). RFESPA-190 cantilevers (Bruker, USA) with a nominal elastic constant of 35 N/m and a typical tip radius of 8 nm were used. The nominal resonance frequency of the cantilevers (provided by the manufacturer) was 190 kHz and the typical operating resonance frequency was 157.4 kHz. AFM images were scanned at 512 × 512 or 1024 × 1024 pixel resolution at 0.8 Hz. To avoid defects and imperfections, a regime of weak tip-sample interaction was applied during scanning by monitoring the tip dithering phase shift. AFM images were processed by subtracting the polynomial fit from each scan line independently then the height images were fed to cross sections using JPKSMP data processing software (Bruker, USA).

FLIM measurements

Time-resolved imaging experiments were conducted employing a MicroTime 200 microscope system purchased from PicoQuant (GmbH, Berlin, Germany). The samples were excited with 405 nm solid-state laser (Picoquant) with pulses characterized by a full width at half maximum (FWHM) of less than 90 ps. This wavelength of laser light was chosen to specifically excite the 0-0 vibrational maximum of the main electronic absorption band of AmB. The laser light beam was directed at the sample through an Olympus 60x objective with a numerical aperture of 1.2. The resulting fluorescence emission was collected by the same objective and transmitted to an avalanche photodiode detector (Excelitas Technologies) configured in a confocal mode. The detection efficiency of the detector was up to 70% at 500 nm, with a timing resolution down to <250 ps (FWHM). A pinhole diameter of 50 μm was utilized, and scattered light underwent filtration through a long-wavelength pass filter HQ430lp followed by a dichromatic mirror ZT405RDC, both sourced from AHF Analysentechnik.

The analysis of fluorescence components was executed utilizing SymPhoTime v. 2.8 software (PicoQuantGmbH, Berlin, Germany). This analytical process encompassed the identification of components based on characteristic fluorescence lifetime values (τ_i) derived from the emission intensity formula *I(t)*:

$$I(t) = \int_{-\infty}^{t} IRF(t') \sum_{i=1}^{n} A_i \, e^{-\frac{t-t'}{\tau_i}} dt' + Bkgr$$

Wherein, *t* represents time, *IRF(t')* denotes the instrument response function at a reference time *t'*, *n* is the number of exponentials, A_i signifies exponential prefactors, and *Bkgr* accounts for background correction.

Subsequently, intensities associated with each exponential component, reflecting non-zero contributions from distinct organizations of fluorophores, were computed:

$$I(i) = \tau_i \mathrm{A}_i$$

These intensities were indicative of the quantity of distinct molecular organizations of the antibiotic. Additionally, the amplitudes associated with the intensities were expressed as a percentage referenced to the total intensity.

Selected monomolecular film regions 10 x 10 μm or 20 x 20 μm were scanned at a resolution of 300 x 300 pixels. The optical resolution of the microscope, considering the specified objective parameters and excitation wavelength, enabled the discrimination of structures with a minimum dimension of 226 ± 27 nm.

The fluorescence signal from the bright spots observed in the microscopic images was extracted through the exit port of the microscope system and subsequently directed into a spectrograph for further analysis. To ensure the fidelity of the collected data and eliminate interference from Raman and Rayleigh scattered light, a long-wavelength pass filter (HQ430lp) was employed prior to detection (the same as used to record images). Spectral data were recorded using a spectrograph model SR 163 (Shamrock), which was equipped with a Newton 970 EMCCD camera from Andor Technology (detection efficiency of up to 95%). The camera was thermoelectrically cooled down to -60°C to minimize noise during data acquisition, thereby ensuring high-quality signal capture. The SR 163 spectrograph, employing a Czerny Turner design with a grating having 600 lines per millimeter, blazed at 500 nm, enabled the acquisition of fluorescence spectra across a spectral window of 250 nm. Data were recorded and processed using Solaris software, with exposure time (20 s) optimized to maximize signal-to-noise ratio. Subsequent statistical analyses were performed using established statistical tools implemented to Grapher program (Golden Software) to derive meaningful insights from the collected data.

All types of experiments, including AFM and FLIM imaging for different monolayers, were repeated at least 10 times and found to be reproducible.

REFERENCES

(1) Grela, E.; Wieczor, M.; Luchowski, R.; Zielinska, J.; Barzycka, A.; Grudzinski, W.; Nowak, K.; Tarkowski, P.; Czub, J.; Gruszecki, W. I. A mechanism of binding of an antifungal antibiotic amphotericin B to lipid membranes: An insight from combined single membrane imaging, micro-spectroscopy, and molecular dynamics. *Mol. Pharm.* **2018**, *15*, 4202−4213.

(2) Gagos, M.; Gabrielska, J.; Dalla Serra, M.; Gruszecki, W. I. Binding of antibiotic amphotericin B to lipid membranes: monomolecular layer technique and linear dichroism-FTIR studies. *Mol. Membr. Biol.* **2005**, *22* (5), 433-442.

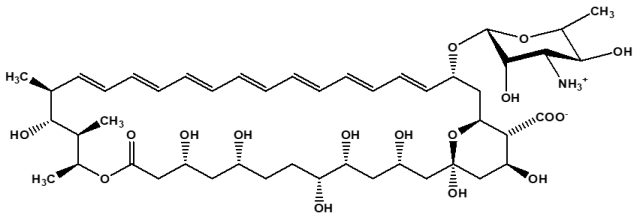

Figure S1 Chemical structure of amphotericin B.

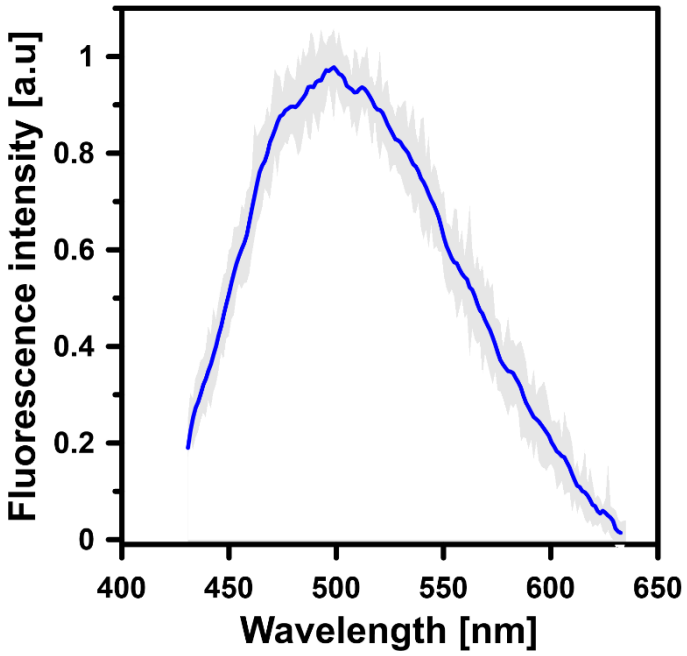

Figure S2 Fluorescence emission spectrum of AmB incorporated in a monomolecular layer composed of DOPC:Ergo (7:3, mol:mol). The spectrum (plotted in blue) represents the arithmetic mean of 16 individual, single-pixel spectra recorded from different fluorescence-emitting structures visible in the FLIM image. The gray area represents S.D. from the arithmetic mean. The spectra were recorded from a monolayer deposited on the mica surface.

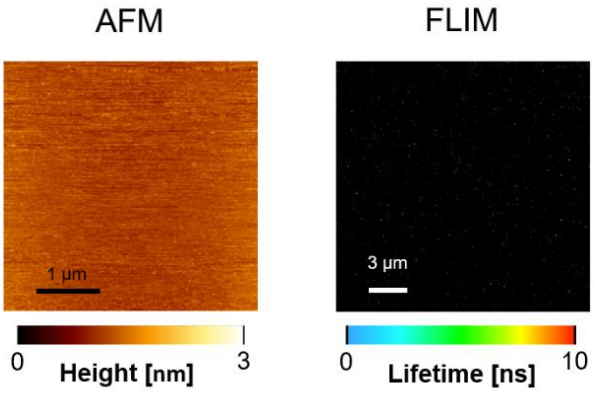

Figure S3 Images acquired with AFM and FLIM (indicated) of the same film deposited from a monomolecular layer formed with DOPC (without Ergo) and exposed to AmB. Note the lack of a signal assigned to AmB.

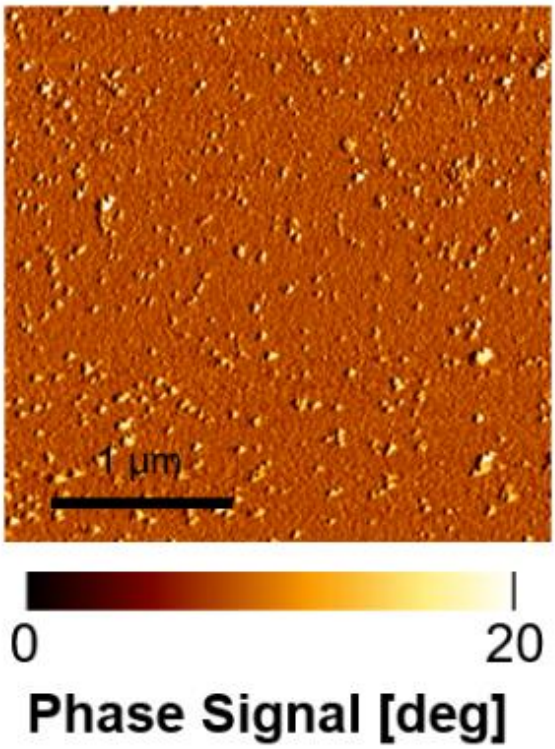

Figure S4 AFM image of the film deposited from the monomolecular layer composed of DOPC and Ergo (7:3, mol:mol) exposed to AmB. The image is based on a phase signal reflecting the mechanical properties of scanned objects.

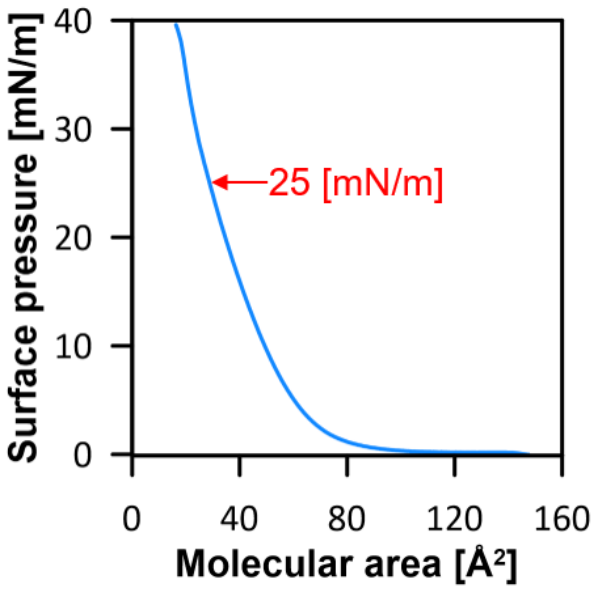

Figure S5 Surface pressure-mean molecular area isotherm of compression of a two-component monomolecular layer formed with DOPC:Ergo (7:3, mol:mol) at the air-water interface. In order to expose a monolayer to AmB, compression was stopped and stabilized at 25 mN/m, while AmB solution was injected into the aqueous subphase.